Coverage Dependence of CO Surface Diffusion on Pt Nanoparticles: An EC-NMR Study

Takeshi Kobayashi, Panakkattu K. Babu, Jong Ho Chung, Eric Oldfield,* and Andrzej Wieckowski*

Department of Chemistry, University of Illinois at Urbana-Champaign, 600 South Mathews Avenue, Urbana, Illinois 61801

Received: October 16, 2006; In Final Form: February 20, 2007

We have studied the effects of CO surface coverage on the diffusion rates of CO adsorbed on commercial Pt-black in sulfuric acid media by using ^{13}C electrochemical nuclear magnetic resonance (EC-NMR) spectroscopy in the temperature range 253−293 K. The temperature range chosen for these measurements was such that the electrolyte is in a liquid-like and liquid environment. For CO coverage between $\theta = 1.0$ and 0.36, the CO diffusion coefficients (D_{CO}) follow a typical Arrhenius behavior and both the activation energies (E_d) as well as the pre-exponential factors (D^0_{CO}) show CO coverage dependence. For partially CO covered samples, E_d decreases linearly with increasing CO coverage, indicating that the repulsive CO−CO interactions exert a stronger influence on the coverage dependence of the activation energy than does the nature of the CO adlayer structure. On the other hand, D^0_{CO} shows an exponential decrease with increasing CO coverage, consistent with the free site hopping model [Gomer, R. *Rep. Prog. Phys.* **1990**, *53*, 917] as the major mechanism for surface diffusion of CO at partial coverages, unlike the situation found with a fully CO covered surface [Kobayashi et al., *J. Am. Chem. Soc*., **2005**, *127*, 14164]. Overall, these results are of interest since they improve our understanding of the surface dynamics of molecules at electrochemical interfaces, and may help facilitate better control of fuel cell reactions in which the presence of surface CO plays a crucial role in controlling electrocatalytic reaction rates.

Introduction

Information on the surface diffusion of adsorbed molecules is of fundamental importance since it can lead to important correlations between the adlayer structure and the reactivity at the electrode surfaces.[1] CO diffusion on Pt surfaces has been extensively investigated under ultrahigh vacuum or gas-phase conditions.[2−6] However, prior to our previous report,[7] the surface diffusion of CO on platinum electrodes in an electrochemical environment has not been measured directly, although many estimates have been made, based on indirect methods.[8−10] Electrochemical nuclear magnetic resonance (EC-NMR) spectroscopy is a relatively new technique in electrochemical surface science that permits a detailed study of the electronic structure of electrodes and adsorbates (at both anodes and cathodes).[11−22] It has a distinct advantage over many other surface science techniques that nanoparticle catalysts can be investigated, and the NMR parameters (spectra and relaxation rates) obtained can be readily interpreted in terms of the Fermi level local density of states (E_f-LDOS). Additionally, in the case of adsorbed small molecules, surface diffusion constants can be determined. In previous work,[7] we reported measurement of CO surface diffusion on a nanoparticle Pt electrode saturated with CO (i.e., at a CO coverage, θ, close to 1), and we proposed that surface diffusion was due to CO exchange between different surface sites, driven by the chemical potential gradient.[7] However, the determination of CO diffusion rates for partially CO covered surfaces is of arguably even more importance in the context of more commonly encountered electrochemical conditions, such as those occurring in direct methanol oxidation fuel cells.[8] For instance, the roles of CO coverage-dependent lateral interactions,[23] as well as the CO adlayer structure[24,25] in determining the rates of CO surface diffusion, are not clearly understood. We have therefore carried out a detailed study of the effects of CO surface coverage on the activation barriers for CO diffusion, as well as on the pre-exponential factors. We also make a comparison between our NMR measurements of surface diffusion with those estimated from CO oxidation current transient measurements.[8]

Experimental

Sample Preparation and CO Dosing Procedure. About 300 mg of fuel cell grade polycrystalline platinum black (Johnson-Matthey, MA) was electrochemically cleaned in 0.5 M H_2SO_4 in D_2O (99% enriched, SIGMA-Aldrich) by voltammetric cycling and by holding the electrode potential at 0.46 V (vs RHE, see below) for 15 min.[26] As estimated from TEM,[7] the average diameter of the Pt-black sample used in this study was 7 ± 2 nm. After the cleaning procedure was completed, CO adlayers were produced either by bubbling ^{13}C (99%) enriched CO (Cambridge Isotopes, MA) through the electrolyte, or by catalytic decomposition of ^{13}C-enriched methanol. As already documented, the type of chemisorbed CO on platinum does not depend on the source of CO.[27] To prepare the sample with $\theta = 1.0$ (saturation coverage of CO) and $\theta = 0.68$, ^{13}CO was adsorbed by admitting the gas to the electrolyte at an open circuit potential (ca. 0.2 V after CO adsorption), followed by purging the electrolyte with ultrapure argon, to remove excess CO.[7] (The duration of CO admission was adjusted to get to the coverage near 0.7 ML.) To prepare CO−Pt samples at $\theta < 0.5$, ^{13}C [99%]-enriched methanol (Cambridge Isotopes, MA) was directly decomposed on the Pt catalysts.[17] The sample with θ

* Corresponding authors. Emails: eo@chad.scs.uiuc.edu; andrzej@scs.uiuc.edu.

10.1021/jp066803b CCC: $37.00
Published on Web 04/21/2007

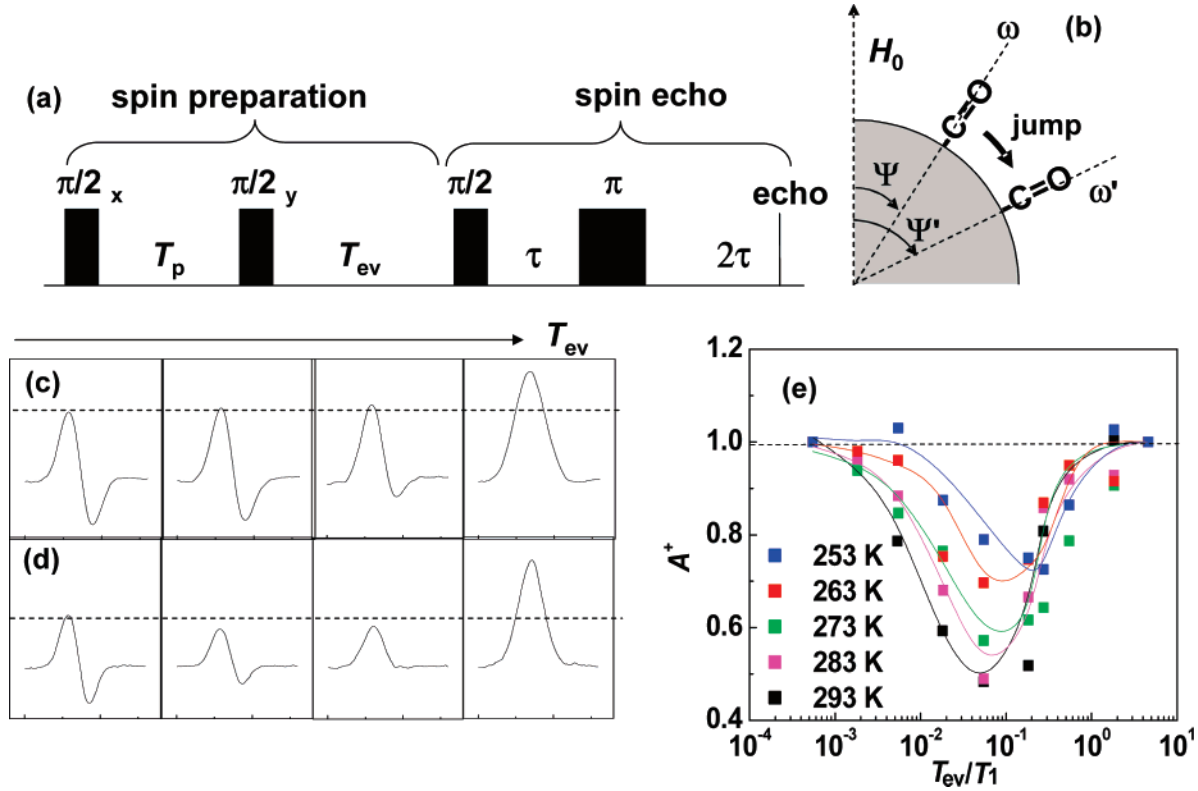

Figure 1. (a) The S-shape pulse sequence, based on ref 28. (b) Schematic diagram of CO surface diffusion altering the ^{13}C Larmor frequency (ω). (c, d) NMR line shapes obtained for the S-shape pulse sequence and their evolution with T_{ev}. (c) At 120K (no diffusion), the amplitude of the positive part, $M^+(T_{ev})$, grows back monotonically to its thermal equilibrium and (d) At 293 K (fast diffusion), the amplitude $M^+(T_{ev})$ initially decreases due to the mixing of noninverted and inverted spin magnetization, as a result of surface diffusion. (e) Variation of A^+ in the S-shape experiment for the $\theta = 0.46$ sample. At $T = 120$ K, $A^+ = 1$ for all T_{ev} values, showing no mixing of inverted and noninverted spins. At $T = 293$ K, $A^+ < 1$, due to spin mixing.

$= 0.46$ was prepared by holding the potential at 0.4 V for 4 h in a solution of 100 mM methanol in 0.5 M H_2SO_4. For preparing the sample with $\theta = 0.36$, Pt catalysts were held at 0.4 V for 16 h in a solution of 2 mM methanol in 0.5 M H_2SO_4. At the end of the CO adsorption cycles (from methanol), excess electrolyte plus methanol was removed and the cell was refilled with 0.5 M D_2SO_4. This rinsing procedure was repeated six times. The NMR samples were transferred to glass ampoules along with the electrolyte and then flame sealed.[16] A small amount of sample was left in the electrochemical cell, to permit the determination of CO coverages. These coverages were estimated from the CO oxidation charge on CO stripping voltammetry, assuming that the oxidation of a CO monolayer requires 420 μC cm^{-1} of Pt, with respect to hydrogen adsorption charge (210 μC cm^{-1} of Pt). Since CO desorption from Pt surfaces and CO migration between nanoparticles is known to be negligible, we do not expect any variations in CO coverage between different particles. All potentials are referenced with respect to the reversible hydrogen electrode, RHE.

NMR Experiments. We use the "S-shape" pulse sequence (Figure 1a) for the measurement of CO surface diffusion. As described elsewhere,[7,28] this sequence consists of a spin echo sequence preceded by a selective inversion sequence. Part of the spins are inverted by the first two 90° pulses and are then allowed to diffuse on the surface during the evolution period, T_{ev}. The surface diffusion of a CO molecule can alter the relative orientation between the ^{13}CO's molecular axis and the external magnetic field (Figure 1b) which changes the ^{13}C spin's Larmor frequency. This will lead to a change in the net nuclear magnetization, which can be monitored through intensity changes in the NMR spectrum. When adsorbed CO molecules do not undergo any surface diffusion, the non-inverted part of the magnetization, and hence the normalized signal amplitude ($M^+(T_{ev})$), grows back monotonically to its thermal equilibrium value with increasing T_{ev}, as shown in Figure 1c. However, if CO molecules undergo surface diffusion during T_{ev}, then the mixing of the inverted and non-inverted spin magnetization leads to an initial decrease in the amplitude $M^+(T_{ev})$ of the non-inverted part of the spectrum (Figure 1d) before it grows back to its thermal equilibrium value. $M^+(T_{ev})$ is measured experimentally for various values of T_{ev} and then compared with a theoretically calculated $M^+(T_{ev})$ value, assuming no diffusion contributions. In order to calculate the diffusion coefficient (D_{CO}), we follow a normalized signal amplitude, A^+, defined as a ratio of [$M^+(T_{ev})$ with diffusion]/[$M^+(T_{ev})$ without diffusion], as a function of T_{ev}. The contribution due to the mixing of inverted and noninverted spins resulting from surface diffusion of CO can be seen as a trough in the A^+ values when plotted against T_{ev}/T_1, Figure 1e. More details of the extraction of the diffusion constant/activation barriers can be found elsewhere.[28]

^{13}C NMR measurements were carried out at 8.47 T using a "home-built" NMR spectrometer.[29] Typical 90° pulse widths of 8−12 μs and a 30 μs delay were used for echo detection. The T_p value (Figure 1a) used in all cases was 8 μs, while T_{ev} was varied from 80 μs to 1.5 s. ^{13}C T_1 values were obtained by using an inversion−recovery technique. Experiments were carried out between 253 and 293 K at 10 K intervals using a continuous flow cryostat (CF-1200, Oxford Instruments, MA) on four samples of CO adsorbed on Pt-black, having coverages of $\theta = 1.0$, 0.68, 0.46, and 0.36. The ^{13}C NMR signal showed a broad, single Gaussian peak and there was no indication of

TABLE 1: Surface Diffusion Parameters (E_d and D^0_{CO}) for CO on Platinum, and the CO Diffusion Coefficient (D_{CO}) at the Temperature of 293 K as a Function of Converge in Various Environments

sample	θ	E_d (kcal/mol)	D^0_{CO} (cm^2/s)	D_{CO} (cm^2/s)	ref
			In Electrolyte		
Pt black (ca. 7 nm)	1.00[a]	6.0 ± 0.4	$(1.1 \pm 0.7) \times 10^{-8}$	3.6×10^{-13}	7
	0.68[a]	6.7 ± 0.6	$(4.8 \pm 2.3) \times 10^{-8}$	8.1×10^{-13}	this work
	0.46[a]	8.0 ± 0.8	$(8.8 \pm 4.0) \times 10^{-7}$	9.5×10^{-13}	this work
	0.36[a]	8.4 ± 0.8	$(3.7 \pm 1.9) \times 10^{-6}$	1.5×10^{-12}	this work
Pt black (8 nm)	~0.5[a]	7.9 ± 2.0			14
Pt/GC (3.1 nm)[b]	0.65−0.75[c]			3×10^{-14}	47
Pt/GC (1.7 nm)[b]	0.8~0.93[c]			7×10^{-17}	47
			In Gas/UHV		
Pt/Al_2O_3 (10 nm)	0.5	6.5 ± 0.5	6×10^{-7}		28
Pt(111)	0.1	4.7 ± 0.1	$(1.4 \pm 0.4) \times 10^{-6}$		6
Pt(111)	0.67	3.0 ± 0.1	$(4.5 \pm 1.0) \times 10^{-7}$		6

[a] θ_{CO} was estimated from CO oxidation charge on cyclic voltammetry, with respect to hydrogen adsorption. [b] Electrochemical measurements. [c] θ_{CO} was deduced from CO oxidation at constant potential.

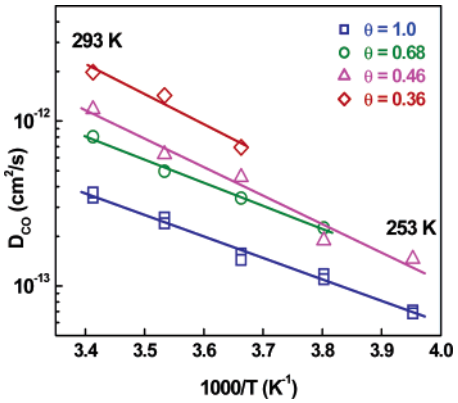

Figure 2. Variation of the diffusion coefficients with temperature for different CO coverages, θ. Straight lines correspond to the Arrhenius fits which yield the activation energies and pre-exponential factors given in Table 1.

any CO present in the electrolyte, which would have resulted in a sharp resonance at ~181 ppm. The chemical shifts for ^{13}C are reported with respect to tetramethylsilane (TMS) using the IUPAC δ-scale in which high frequency, low-field, paramagnetic or deshielded values are positive.

CO Electrooxidation Measurements. A three-electrode electrochemical cell was used for the electrochemical measurements and consists of a Pt wire counter electrode, a 3 M NaCl Ag/AgCl reference electrode and a working electrode, constructed by depositing a Pt sample suspension onto a 12 mm diameter polished gold electrode.[26] The Pt sample suspension was obtained by adding the Pt-black samples to Milli-Q water, followed by sonication. The resulting suspension was dropped onto the polished gold electrode, then dried under a heating lamp. After rinsing, the catalyst film was mechanically stable and the Pt nanoparticles showed voltammetric behavior very similar to that seen previously, with polycrystalline samples.[26] The cell potential was controlled by a potentiostat (AUTOLAB, Echo Chemie, Netherlands). A 0.1 M H_2SO_4 solution was prepared from analytical grade sulfuric acid, diluted in Millipore water. A CO adlayer was produced by holding the electrode potential at 0.100 V for 15 min under CO bubbling, followed by purging the solution with ultrapure argon for 35 min, at the same potential. The potential was then stepped to a value in the range 0.730−0.800 V, and current transients recorded. CO diffusion coefficients (at room temperature) were estimated from these current transients by using the method described by Maillard et al.[8] This model is based upon several assumptions, one of them being that the diffusion coefficient is independent of CO surface coverage.[8] We discuss this topic in more detail below, in light of the EC-NMR observations.

Results and Discussion

NMR Measurement of Diffusion Parameters. Becerra et al.[28] were the first to use the "S-shape" pulse sequence employed in this study, measuring diffusion of CO adsorbed on alumina-supported Pt nanoparticles under "gas phase" conditions. They reported diffusion parameters for samples with three different Pt dispersions and two different CO surface coverages.[28] The activation energies for surface diffusion (E_d) were found to lie in the range 6.5−10.5, kcal/mol and a typical value of the pre-exponential factor, D^0_{CO}, was $\sim 6 \times 10^{-7}$ cm^2s^{-1}. The activation energy increased from 7.4 to 10.5 kcal/ mol when the Pt dispersion was increased from 23% to 73%. Though both E_d and D^0_{CO} changed with CO coverage, no systematic variations could be inferred from this gas phase study.[28]

In contrast to these results, we find here a strong dependence for E_a and D_{CO} on surface coverage, as shown in Table 1. When the D_{CO} results are plotted as a function of T^{-1} for the four different CO coverages (Figure 2), we find in each case typical Arrhenius behavior, $D_{CO} = D^0_{CO} \exp(-E_d/RT)$, where (as per above) D^0_{CO} is the pre-exponential factor and E_d is the activation energy for CO diffusion. Moreover, it can also be seen from Figure 2 that D^0_{CO}, E_d and D_{CO} are all dependent on CO surface coverage. More specifically, the activation energy increases from 6.0 to 8.4 kcal/mol while the pre-exponential factor increases from 1.1×10^{-8} to 3.7×10^{-6}, when the CO surface coverage is reduced from $\theta = 1.0$ to $\theta = 0.36$. For purposes of comparison, the Arrhenius parameters previously obtained for CO adsorbed and measured in the gas phase on supported Pt catalysts,[28] and on a single crystal in UHV,[7] are also shown in Table 1. When the CO coverage is reduced from $\theta = 1$ to 0.68, E_d increases from 6.0 to 6.7 kcal/ mol. With further decreases in CO coverage ($\theta = 0.46$ and 0.36), the activation energy increases to ~8.0 kcal/mol. The E_d values (6−6.7 kcal/mol) for the high coverage samples ($\theta = 1.0$ and 0.68) compare well with 6.5 kcal/mol, the E_d value reported for CO diffusion on alumina-supported Pt in gas phase at $\theta = 0.5$.[28] In this gas-phase experiment as well as in some other UHV investigations, the activation energy for CO surface diffusion was reported to be coverage dependent.[6,28,30]

In Figure 3, we show the coverage dependence of the diffusion parameters. For partial coverages, E_d decreases linearly (Figure 3a) and D^0_{CO} decreases exponentially (Figure 3b) with increasing coverage. E_d value extrapolated to the zero coverage

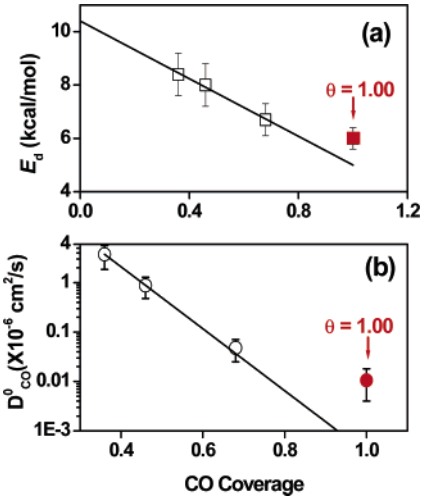

Figure 3. Coverage dependence of CO diffusion parameters. (a) Variation of the activation energy with CO coverage. The straight line corresponds to Frumkin-type behavior for the partially covered samples. (b) Variation of the pre-exponential factor with CO coverage. The exponential fit (solid line) suggests that for the partially covered samples ($\theta < 1$), free-site hopping is the principal surface diffusion mechanism. The experimental points corresponding to full coverage ($\theta = 1$) are shown in red and indicate that the diffusion mechanism for CO at $\theta = 1$ is qualitatively different from the free site hopping model, applicable at partial coverage.

limit provides the Gibbs free energy of activation for diffusion at zero coverage ($\Delta G_{\theta=0}$), and the slope of the fit gives the Frumkin interaction parameter, r.[31] From the straight line fit (Figure 3a) we obtain a $\Delta G_{\theta=0}$ value of 10.4 ± 1.6 kcal/mol, about twice as large as the $\Delta G_{\theta=0}$ obtained for CO on Pt (111) under UHV conditions.[6] This observation implies that additional morphological features, like edges and defects on the nanoparticle surfaces (see below), as well as the presence of the electrochemical double layer, may hinder the surface diffusion of adsorbed CO in an electrochemical environment. Moreover, the large negative value for the Frumkin interaction parameter ($r = -5.4 \pm 2.9$ kcal/mol), clearly indicates that repulsive CO−CO interactions dominate the coverage dependence of E_d.

Though the E_d versus CO coverage relationship we observe is basically similar to that seen with single crystal planes in UHV,[6,32] the actual magnitude of E_d for the nanoparticle surfaces is likely to depend on the binding energy variations among different adsorption sites.[6] When CO is preferentially adsorbed at edges or corner sites (where its binding energy is large), its mobility is low. At lower coverages, the fraction of CO adsorbed on such sites is high, leading of course to a higher activation energy.[2] Since the nanoparticles in our system are expected to have a high fraction of edges and corner sites, it appears that such morphological effects may contribute to the large differences in activation energy seen between our Pt nanoparticles and the single-crystal surface results, shown in Table 1. Also, differences in E_d values are observed between nanoparticle surfaces in gas phase and electrochemical environments. For example, the E_d of 8.0 kcal/mol for $\theta = 0.46$ is higher than that measured for CO adsorbed at $\theta = 0.5$ on 10 nm Pt/Al_2O_3 under gas-phase conditions (6.5 kcal/mol),[28] which could be due to the presence of coadsorbed anions in the double layer, as suggested previously.[7,33]

In addition to the effects of defects and lateral interactions, it is also known that CO adsorbed onto Pt surface can occupy either atop or bridge sites, and the ratio of these two populations is a function of coverage.[24,25,34] On a Pt(111) single-crystal surface at room temperature at $\theta < 0.33$, a $(\sqrt{3} \times \sqrt{3})$R30° structure with CO on linear or atop sites (CO_L) is formed (Figure 4a), while at $\theta = 0.5$, a $c(4 \times 2)$ structure (Figure 4b) is obtained, containing both atop and bridge-bonded CO (CO_B).[34−36] For higher coverages, $\theta \approx 0.75$, CO forms a compressed (2×2)−3CO structure (Figure 4c), and the fraction of CO_L species increases.[37,38] Finally, when the coverage is near saturation ($\theta \approx 1$), all CO molecules occupy the atop site (Figure 4d).[39] CO_L is known to have a larger heat of adsorption than CO_B,[40] and so, at low coverage, the adsorbed CO molecules tend to occupy the atop position. However, at coverages of $\theta > 0.33$, the CO−CO repulsive interactions will tend to spread out the CO molecules and, at temperatures >50 K, a fraction of CO molecules can get thermally activated and occupy bridge sites,[41] and CO molecules on bridge sites are thought to be more mobile than are those on atop sites. When surface coverage decreases below 0.33, the CO−CO lateral interactions no longer contribute to the CO binding energy,[41] and if all CO molecules are adsorbed onto edge/corner sites, the activation energy for the surface diffusion is likely to reach a limiting value.

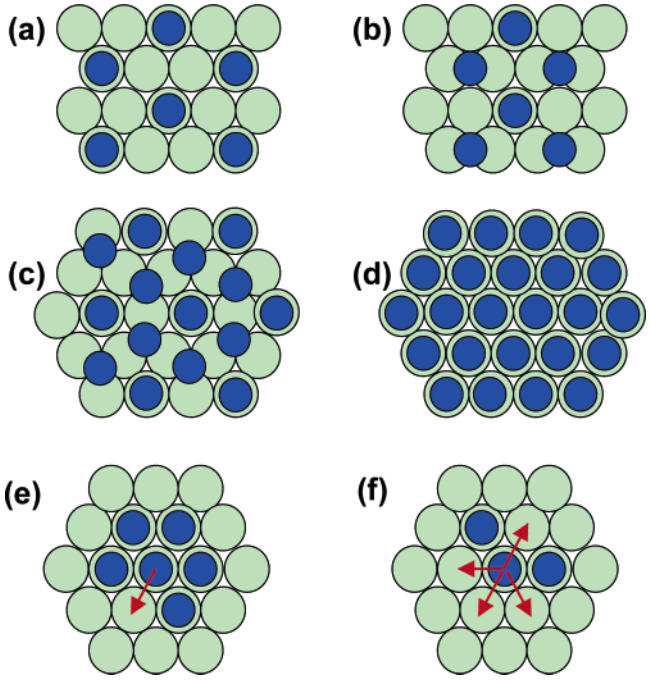

Figure 4. Schematic representation of CO adsorbate structure on platinum: (a) Pt(111)$(\sqrt{3} \times \sqrt{3})R30°$ structure for low coverage ($\theta \approx 0.33$); (b) Pt(111)$c(4 \times 2)$ at around half coverage ($\theta \approx 0.5$), (c) Pt(111)(2×2)-3CO structure at ($\theta \approx 0.75$) and (d) the structure at a saturation coverage where CO is adsorbed exclusively on atop sites. Panels e and f illustration of the free site hopping model where the green and blue circles represent surface Pt sites and adsorbed CO, respectively. CO can move to free adjacent sites as indicated by the red arrows. At high coverage (e), there are less free sites available around a given CO molecule, which results in a smaller pre-exponential factor. Availability of many free sites at low coverage (f) leads to a larger pre-exponential factor.

TABLE 2: Estimates of CO Diffusion Coefficients (Figure 5) Using Electrochemical Model Developed in Ref 8

	diffusion coefficients (cm^2/s)			
sample	730 mV	760 mV	780 mV	800 mV
Pt-black (7 nm)	1.0×10^{-11}	1.5×10^{-11}	1.9×10^{-11}	2.1×10^{-11}

The EC-NMR value of D^0_{CO} of 8.8×10^{-7} cm^2/s for $\theta = 0.46$ is quite close to that for surface diffusion of CO on 10 nm Pt nanoparticles supported on Al_2O_3 at $\theta = 0.5$ (Table 1). The D^0_{CO} value for $\theta = 1.0$ is the smallest in the series (Table 1), and in a previous study,[7] we proposed that surface diffusion

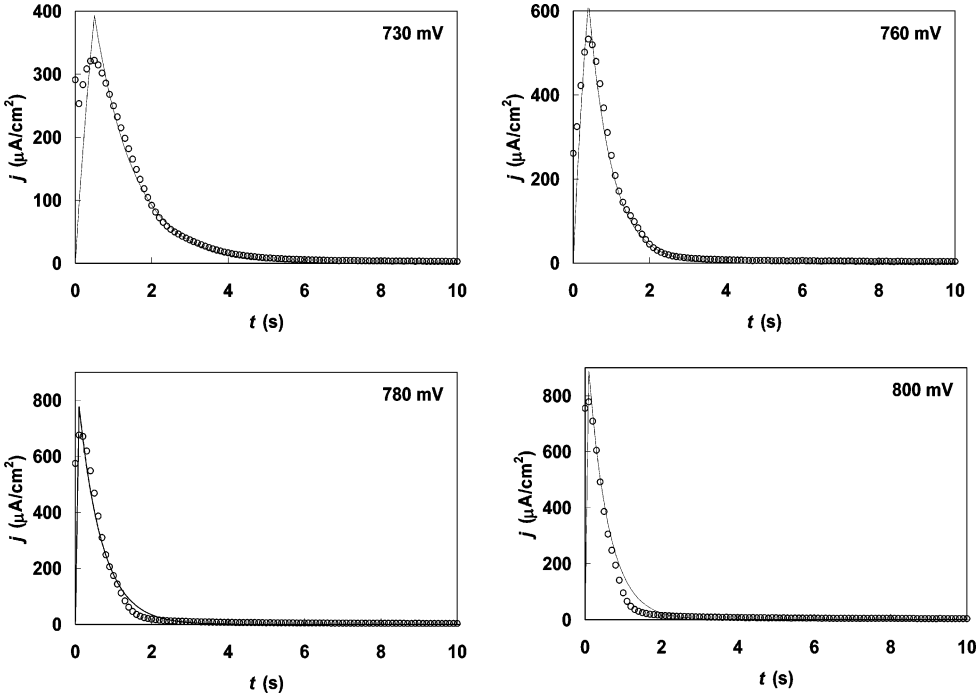

Figure 5. CO oxidation current transients (open circles) obtained after stepping the potentials to 730, 760, 780, and 800 mV vs RHE for a full monolayer of CO adsorbed on Pt-black. The solid lines correspond to the fitted curves calculated by using the "active site" model described in ref 8.

observed on Pt nanoparticle surfaces saturated with CO was due to CO exchange, driven by the chemical potential gradient between different surface sites.[10,42] However, in the present case (nanoparticle Pt partially covered with CO), free site hopping can clearly be a more effective mechanism, in which case, the pre-exponential factor is expected to become a function of CO coverage.[43] The free site hopping mechanism assumes that a diffusing adsorbate stops when a collision takes place with another adsorbate. This collision is assumed to be inelastic, and the collision dissipates the kinetic energy of the diffusing adsorbate. The surface diffusion coefficient is coverage dependent because the collision frequency is higher, and the adsorbate mean free path is lower, at higher coverages. The pre-exponential factor will depend on the probability that a given CO molecule can find free sites in its neighborhood. As shown in Figure 3b, D^0_{CO} shows an exponential decrease with increasing CO coverage for the partially covered samples, and similar behavior has been observed for the coverage dependence of surface diffusion of CO on Ru,[44] where diffusion was attributed to free site hopping.[43]

In Figure 4e,f, we show a schematic representation of the free site hopping model. For lower CO coverage (Figure 4f), since there are many free sites on the surface, there is a higher probability that a given CO molecule can find an adjacent vacant site. Consequently, surface diffusion at such lower coverages shows a relatively large pre-exponential factor (Table 1). So although the activation energy for diffusion increases with decreasing coverage, the exponential increase in the pre-exponential factor (resulting from the increased availability of free sites on the surface) results in an overall increase in the diffusion coefficient, from 3.6×10^{-13} at $\theta = 1.0$ to 1.5×10^{-12} cm^2/s at $\theta = 0.36$.

The above results clearly indicate that adsorbate coverage is a significant factor in surface diffusion events, at least in the coverage range and on the nanoparticle surfaces where the NMR experiments were carried out. It can also be seen that E_d as well as D^0_{CO} at $\theta = 1.0$ do not fall on the solid lines, consistent with our previous suggestion[7] that the surface diffusion mechanism for fully CO covered samples is qualitatively different, as discussed above.

Electrochemical Estimation of Diffusion Parameters. We next compare the EC-NMR results with those obtained electrochemically by using the protocol described by Maillard et al.[8] in which CO diffusion coefficients are estimated from potentiostatic CO monolayer oxidation transients (Table 2). We show in Figure 5 the current transients (circles) for the oxidation of CO adlayers ($\theta = 1.0 \pm 0.01$) recorded after stepping the potential from 0.100 V to the potentials indicated. The transients were recorded up to 100∼300 s then a background current was subtracted. However, applying the model described previously[8] gives much higher diffusion coefficient, values in the range of 10^{-11} cm^2/s, to be compared with the 3.6×10^{-13} cm^2/s value found in the NMR studies (Table 1). This result casts doubts on the applicability of the electrochemical model for deducing surface diffusion rates on the large nanoparticle Pt black surfaces used in this study. Indeed, Andreaus et al.[45] concluded that due to the high mobility of CO adsorbed on larger nanoparticles (>4 nm), surface diffusion was no longer the rate-limiting factor for the CO oxidation process, in accord with our observations.

Electrochemical modeling of surface diffusion assumes that the diffusion coefficient is independent of surface coverage.[8,46] However, the NMR result for D_{CO} at $\theta = 0.36$ is an order of magnitude larger than that at $\theta = 1.0$, clearly demonstrating that the diffusion coefficient is coverage-dependent (Table 1). This observation points to a crucial difference between the NMR and electrochemical measurements: during the NMR experiment, there is no change in CO coverage, whereas the electrochemical experiment represents a dynamical situation in which CO surface coverage undergoes a continuous decrease. The NMR method is, therefore, a unique experimental probe with which to accurately determine surface diffusion on nanoparticle catalysts and could prove to be particularly valuable in theoretical modeling of the dynamics of chemisorbed species in electrochemical environments.

Conclusions

We have applied the EC-NMR technique to investigate the effects of surface coverage on the diffusion parameters of CO adsorbed on Pt-black in an electrochemical environment in a temperature range where the electrolyte is in liquid-like and liquid state. CO diffusion coefficients for all samples follow Arrhenius behavior and the diffusion parameters show coverage-dependence. For partially covered samples, the activation energy increases linearly and the pre-exponential factor increases exponentially with decreasing coverage, suggesting that CO coverage is a significant factor in determining the diffusion rates. Although E_d increases with decreasing coverage, the exponential increase in D^0_{CO}, due to the availability of more free surface sites, leads to a larger CO diffusion coefficient at lower coverages. The exponential variation of D^0_{CO} for partial CO coverage samples confirms free site hopping as the major diffusion mechanism. The large negative value for the Frumkin interaction parameter indicates that repulsive CO−CO interactions have a stronger influence on the coverage dependence of E_d than does the nature of the adlayer structure. The present investigation also suggests that coverage dependence must be considered when investigating surface reactions involving diffusive motions of adsorbates as the elementary step, and should therefore be included in surface electrochemical rate modeling calculations.

Acknowledgment. The authors wish to thank the reviewers of this paper for their helpful comments. This work is supported by the National Science Foundation under Grant CHE 03-49999 and by the Army Research Office under MURI contract DAAD19-03-1-0169 granted to AW, for fuel-cell research in collaboration with Case Western Reserve University.

References and Notes

(1) Earis, P., Ed.; The Dynamical Electrode Surface. *Faraday Discuss.* **2002**, *119*, 121.
(2) Poelsema, B.; Verheij, L. K.; Comsa, G. *Phys. Rev. Lett.* **1982**, *49*, 1731.
(3) Reuttrobey, J. E.; Doren, D. J.; Chabal, Y. J.; Christman, S. B. *J. Chem. Phys.* **1990**, *93*, 9113.
(4) Reuttrobey, J. E.; Doren, D. J.; Chabal, Y. J.; Christman, S. B. *Phys. Rev. Lett.* **1988**, *61*, 2778.
(5) Vonoertzen, A.; Rotermund, H. H.; Nettesheim, S. *Surf. Sci.* **1994**, *311*, 322.
(6) Ma, J. W.; Xiao, X. D.; DiNardo, N. J.; Loy, M. M. T. *Phys. Rev. B* **1998**, *58*, 4977.
(7) Kobayashi, T.; Babu, P. K.; Gancs, L.; Chung, J. H.; Oldfield, E.; Wieckowski, A. *J. Am. Chem. Soc.* **2005**, *127*, 14164.
(8) Maillard, F.; Eikerling, M.; Cherstiouk, O. V.; Schreier, S.; Savinova, E.; Stimming, U. *Faraday Discuss.* **2004**, *125*, 357.
(9) Cherstiouk, O. V.; Simonov, P. A.; Zaikovskii, V. I.; Savinova, E. R. *J. Electroanal. Chem.* **2003**, *554*, 241.
(10) Lebedeva, N. P.; Koper, M. T. M.; Feliu, J. M.; van Santen, R. A. *J. Phys. Chem. B* **2002**, *106*, 12938.
(11) Babu, P. K.; Chung, J. H.; Kuk, S. T.; Kobayashi, T.; Oldfield, E.; Wieckowski, A. *J. Phys. Chem. B* **2005**, *109*, 2474.
(12) Babu, P. K.; Kim, H. S.; Oldfield, E.; Wieckowski, A. *J. Phys. Chem. B* **2003**, *107*, 7595.
(13) Babu, P. K.; Oldfield, E.; Wieckowski, A. Nanoparticle Surface Studied by Electrochemical NMR. In *Modern Aspects of Electrochemistry*; Vayenas, C., Ed.; Kluwer Academic/Plenum Publishers: New York, 2003; Vol. 36, p 1.
(14) Day, J.; Vuissoz, P.-A.; Oldfield, E.; Wieckowski, A.; Ansermet, J.-P. *J. Am. Chem. Soc.* **1996**, *118*, 13046.
(15) Slezak, P. J.; Wieckowski, A. *J. Mag. Reson.* **1993**, *A 102*, 166.
(16) Tong, Y. Y.; Belrose, C.; Wieckowski, A.; Oldfield, E. *J. Am. Chem. Soc.* **1997**, *119*, 11709.
(17) Tong, Y. Y.; Kim, H. S.; Babu, P. K.; Waszczuk, P.; Wieckowski, A.; Oldfield, E. *J. Am. Chem. Soc.* **2002**, *124*, 468.
(18) Tong, Y. Y.; Oldfield, E.; Wieckowski, A. *Anal. Chem.* **1998**, *70*, A 518.
(19) Tong, Y. Y.; Rice, C.; Godbout, N.; Wieckowski, A.; Oldfield, E. *J. Am. Chem. Soc.* **1999**, *121*, 2996.
(20) Tong, Y. Y.; Rice, C.; Wieckowski, A.; Oldfield, E. *J. Am. Chem. Soc.* **2000**, *122*, 11921.
(21) Tong, Y. Y.; Wieckowski, A.; Oldfield, E. *J. Phys. Chem. B* **2002**, *106*, 2434.
(22) Vuissoz, P. A.; Ansermet, J. P.; Wieckowski, A. *Phys. Rev. Lett.* **1999**, *83*, 2457.
(23) Yeo, Y. Y.; Wartnaby, C. E.; King, D. A. *Science* **1995**, *268*, 1731.
(24) Chang, S.-C.; Roth, J. D.; Ho, Y.; Weaver, M. J. *J. Electron Spectrosc. Relat. Phenom.* **1990**, *54*−*55*, 1185.
(25) Podkolzin, S. G.; Shen, J.; de Pablo, J. J.; Dumesic, J. A. *J. Phys. Chem. B* **2000**, *104*, 4169.
(26) Waszczuk, P.; Solla-Gullon, J.; Kim, H. S.; Tong, Y. Y.; Montiel, V.; Aldaz, A.; Wieckowski, A. *J. Catal.* **2001**, *203*, 1.
(27) Lu, C.; Rice, C.; Masel, R. I.; Babu, P. K.; Waszczuk, P.; Kim, H. S.; Oldfield, E.; Wieckowski, A. *J. Phys. Chem. B* **2002**, *106*, 9581.
(28) Becerra, L. R.; Klug, C. A.; Slichter, C. P.; Sinfelt, J. H. *J. Phys. Chem.* **1993**, *97*, 12014.
(29) Babu, P. K.; Kim, H. S.; Chung, J. H.; Oldfield, E.; Wieckowski, A. *J. Phys. Chem. B* **2004**, *108*, 20228.
(30) Lin, T. S.; Lu, H. J.; Gomer, R. *Surf. Sci.* **1990**, *234*, 251.
(31) Bockris, J. O. M.; Reddy, A. K. N.; Gamboa-Aldeco, M. *Modern Electrochemistry - Fundamentals of Electrodics*; Kluwer Academic: New York, 1998; Vol. 2A.
(32) Gomer, R. *Rep. Prog. Phys.* **1990**, *53*, 917.
(33) Housmans, T. H. M.; Koper, M. T. M. *Electrochem. Commun.* **2005**, *7*, 581.
(34) Kizhakevariam, N.; Jiang, X.; Weaver, M. J. *J. Chem. Phys.* **1994**, *100*, 6750.
(35) Hayden, B. E.; Bradshaw, A. M. *Surf. Sci.* **1983**, *125*, 787.
(36) Steininger, H.; Lehwald, S.; Ibach, H. *Surf. Sci.* **1982**, *123*, 264.
(37) Markovic, N. M.; Grgur, B. N.; Lucas, C. A.; Ross, P. N. *J. Phys. Chem. B* **1999**, *103*, 487.
(38) Villegas, I.; Weaver, M. J. *J. Chem. Phys.* **1994**, *101*, 1648.
(39) Park, S.; Wasileski, S. A.; Weaver, M. J. *J. Phys. Chem. B* **2001**, *105*, 9719.
(40) Curulla, D.; Clotet, A.; Ricart, J. M.; Illas, F. *J. Phys. Chem. B* **1999**, *103*, 5246.
(41) Persson, B. N. J.; Tushaus, M.; Bradshaw, A. M. *J. Chem. Phys.* **1990**, *92*, 5034.
(42) Lazar, P.; Schollmeyer, H.; Riegler, H. *Phys. Rev. Lett.* **2005**, *94*, 116101.
(43) Arena, M. V.; Deckert, A. A.; George, S. M. *Surf. Sci.* **1991**, *241*, 369.
(44) Brown, D. E.; Sholl, D. S.; Skodje, R. T.; George, S. M. *Chem. Phys.* **1996**, *205*, 23.
(45) Andreaus, B.; Maillard, F.; Kocylo, J.; Savinova, E.; Eikerling, M. *J. Phys. Chem. B* **2006**, *110*, 21028.
(46) Hopstaken, M. J. P.; Niemantsverdriet, J. W. *J. Chem. Phys.* **2000**, *113*, 5457.
(47) Maillard, F.; Eikerling, M.; Cherstiouk, O. V.; Schreier, S.; Savinova, E.; Stimming, U. *Size Effects on Reactivity of Pt Nanoparticles in CO Monolayer Oxidation: The Role of Surface Mobility*. http://www.rsc.org/ suppdata/FD/b3/b303911k/addition.htm, 2005.